Eur. Phys. J. A **20**, 139–144 (2004)
DOI 10.1140/epja/i2002-10340-1

THE EUROPEAN PHYSICAL JOURNAL A

Rotational bands and alignments in the $1f_{7/2}$ shell

F. Brandolini[a]

Dipartimento di Fisica dell'Università and INFN, Padova, Italy

Received: 31 October 2002 /
Published online: 23 March 2004 –

Abstract. Nuclei in the middle of the $1f_{7/2}$ shell are shown to have rotational features. Dynamic electromagnetic moments have been measured for many transitions. The agreement of large-scale shell model calculations with experimental data is in general excellent. A K-value was assigned to various bands, which can be described in the strong-coupling approximation. Evidence of band crossings is given. The proposed description agrees with observed Coulomb energy differences.

PACS. 21.10.Tg Lifetimes – 23.20.-g Electromagnetic transitions – 23.20.Lv γ transitions and level energies – 27.40.+z $39 \leq A \leq 58$

1 Introduction

A great deal of spectroscopic information, with emphasis on dynamic electromagnetic moments, has been collected in recent years with the γ-spectrometer GASP of LNL for nuclei in the middle of the $1f_{7/2}$ shell: *i.e.* ^{46,47,48}V, ^{48,49,50}Cr, ^{50}Mn and ^{46}Ti [1–7].

This nuclear region turned out to be a very previleged one as Large Scale Shell Model (LSSM) calculations for natural parity states in the full *fp* configuration space get in general an excellent agreement with experimental data [8–10]. This is allowed by the fact that, up to rather high excitation energy, the contribution of the $1d$-$2s$ shell is small, as well as that of the $1g_{9/2}$ orbital.

One main feature is the appearance of rotational features at rather low spin. The mechanism of generating rotational collectivity was explained by the quasi $SU(3)$ model [11], to be mainly due to configuration mixing of the $1f_{7/2}$ with the $2p_{3/2}$ orbital. Unnatural parity sidebands are described by extending the *fp* space to include a nucleon-hole in the $1d_{3/2}$ orbital [12]. Both natural and unnatural parity states become nearly spherical approaching the band termination in the $1f_{7/2}^{n}$ and $2d_{3/2}^{-1} \otimes 1f_{7/2}^{n+1}$ configuration space, respectively. Strongly coupled Nilsson configurations turned out to provide a valid classification criterion at low excitation energy for all rotational bands.

A detailed study of rotational collectivity was systematically made via precise DSAM lifetimes deduced with the procedure named Narrow Gate on Transition Below, which avoids the systematic error due to sidefeeding [13].

Shell model calculations are sometimes not considered able to show transparently the physical characteristics of the nucleus. This is not fully true if one considers that, in order to get a physical interpretation, the calculated electromagnetic moments can be compared with the predictions of collective models. The most used formulas are those related to the rigid rotor.

The intrinsic electric quadrupole moment Q_0 can be derived from the calculated spectroscopic quadrupole moment, according to the formula

$$Q_{\rm s} = Q_0 \frac{3K^2 - I(I+1)}{(I+1)(2I+3)}\,. \tag{1}$$

The intrinsic quadrupole moment can be derived also from the $B(E2)$ values using the formula:

$$B(E2) = \frac{5}{16\pi} Q_{\rm t}^2 \langle I_i K 20 | I_f K \rangle^2 \tag{2}$$

and in this case is denoted as $Q_{\rm t}$.

The values Q_0 and $Q_{\rm t}$ are related to the deformation parameters β and γ via equations

$$Q_0 = \frac{6}{\sqrt{5\pi}} ZeR_0^2 \beta \sin(30+\gamma) \tag{3}$$

and

$$Q_{\rm t} = 2\sqrt{\frac{3}{5\pi}} ZeR_0^2 \beta \cos(30+\gamma)\,. \tag{4}$$

Concerning magnetic properties, for the g-factor one has

$$g = g_R + (g_K - g_R)\frac{K^2}{I(I+1)} \tag{5}$$

and for $M1$ transitions:

$$B(M1) = \frac{3}{4\pi} \langle I_i K 10 | I_f K \rangle^2 (g_K - g_R) K^2 \mu_N^2\,. \tag{6}$$

[a] e-mail: brandolini@pd.infn.it

The very good agreement obtained for all available experimental observables gives rise to a synergy between experiment and theory: the fact that excitation energies and dynamical electromagnetic moments ($M1$ and $E2$) are well reproduced by LSSM legitimates to rely on predicted, but not observed observables, in particular on the static electromagnetic moments, which are very selective probes of the underlying structure of the nucleus.

2 Review of the results

The most deformed nucleus at low excitation energy resulted to be ^{48}Cr [1], which lies exactly in the middle of the shell. Rotational collectivity builds up in the ground-state (gs) band leading to a prolate deformation parameter at low spin ($\beta \simeq 0.30$), which decreases smoothly approaching the spherical band termination at $I = 16^+$, *i.e.* the maximum spin available in the $1f_{7/2}$ configuration space. A backbending is observed at $I = 12^+$, likely due not to a band crossing but to the dominance of configurations with seniority $v = 4$ [14] which is associated to triaxiality. In fact in recent cranked Nilsson-Strutinsky calculations [15], a rather constant prolate deformation is found for spin up to $I = 8^+$, followed by a fast decreasing of β, accompanied by a negative value of gamma which is nearly $-30°$ at $I = 12^+$. According to eq. (3), a much smaller size of Q_s is thus predicted above $I = 10^+$. This agrees with LSSM calculations [8]. The alternative proposal of a band crossing [16] is not tenable since the yrare 12^+ level is predicted nearly 2 MeV higher.

In ^{49}Cr [2,3] LSSM gives, at low excitation energy, an equivalent description to that of the particle-rotor model [17], based on a [312]5/2 neutron configuration. The experimental $B(E2)$ values along the $K^\pi = 5/2^-$ gs band have a similar behaviour as in ^{48}Cr, approaching the $31/2^-$ terminating state, with an important exception for the $25/2^-$ level, whose reduced rates are very small. This is consistent with a "crossing" with a $K^\pi = 13/2^-$ band, which is obtained by exciting a proton from the $[321]3/2^-$ orbital to the $[312]5/2^-$ one and whose bandhead has been observed with the predicted properties [2]. In this description the backbending at $I = 19/2^-$ is not due to a band crossing but to a dominance of states with seniority $v = 3$, in analogy with ^{48}Cr.

A band crossing is predicted also in ^{47}V [3] at the yrast $17/2^-$ level with a $K^\pi = 11/2^-$ band generated by promoting one neutron from the $[321]3/2^-$ orbital to $[312]5/2^-$ one, but its observation is a challenge for future experiments.

In the $Z = N$ nucleus, ^{46}V $K^\pi = 0^+$ and $K^\pi = 3^+$ bands, produced via the parallel and antiparallel coupling of odd nucleons in the $[321]3/2^-$ orbital, are coexisting at low energy [4]. The bands are rather irregular but K-rules work rather well at low spin.

The agreement with theory is spectacular in ^{48}V, where all the members of $K^\pi = 1^+$ and $K^\pi = 4^+$ bands, produced via the parallel and antiparallel coupling of the $\pi[321]3/2^-$ orbital with the $\nu[312]5/2^-$ one, were observed

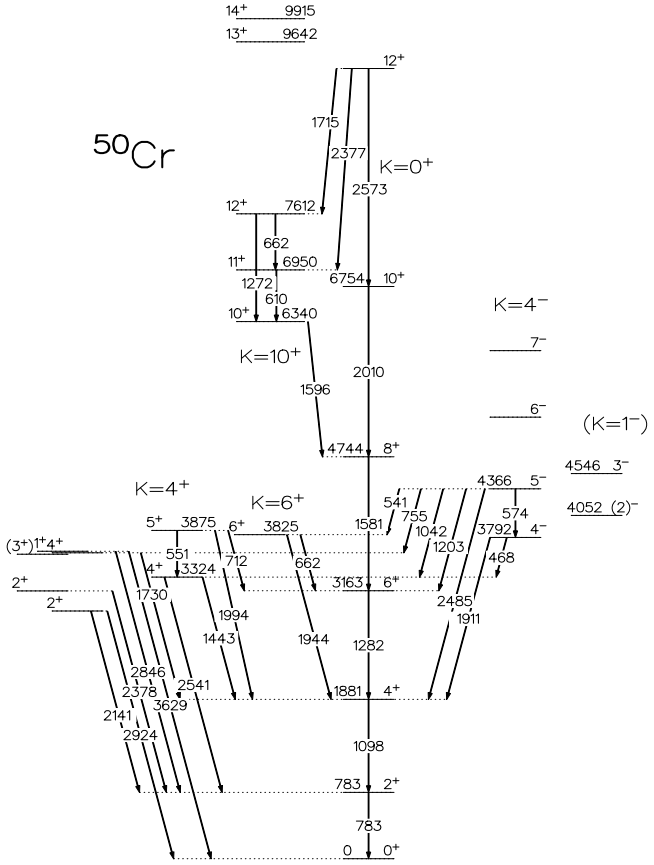

Fig. 1. Partial level scheme of ^{50}Cr.

up to the common band termination [5]. $B(M1)$ reduced rates show a staggering with increasing spin approaching the band termination, which is well accounted by LSSM.

Unnatural parity bands have been extended in ^{46,47,48}V up to the band termination in the $d_{3/2}^{-1} \otimes f_{7/2}^{n+1}$ configuration space and found to have at low spin larger deformation than the gs bands. These bands present shape coexistence and their deformation is maximum in ^{47}V, as it can be described as $d_{3/2}^{-1} \otimes ^{48}$Cr. In ^{46}V, two bands are observed with $K^\pi = 0^-$ and 3^-, respectively, due to the promotion of a nucleon from the $[202]3/2^+$ orbital to the $[321]3/2^-$ one, followed by antiparallel and parallel coupling of the unpaired $[202]3/2^+$ and $[321]3/2^-$ nucleons. Similarly, in ^{48}V, $K^\pi = 1^-$ and $K^\pi = 4^-$ bands are observed, by antiparallel and parallel coupling of the unpaired $[202]3/2^+$ proton and $[312]5/2^-$ neutron. Evidence of band crossing was found in both nuclei with bands $K^\pi = 7^-$ and $K^\pi = 8^-$, respectively, which are due to the excitation of a proton from the $[202]3/2^+$ orbital to the $[321]5/2^-$ one, and a parallel coupling with the $K^\pi = 3^+$ and $K^\pi = 4^+$ gs bands. In ^{48,49,50}Cr, the sidebands were not known before. In ^{49}Cr, two bands with $K^\pi = 3/2^+$ and $13/2^+$ are observed and a crossing occurs at $7/2^+$, so that the latter band acts as a high-K trap. The two bands are described as the coupling of proton $d_{3/2}$-hole to the $K^\pi = 0^+$, $T = 1$ band and to the $K^\pi = 5^+$, $T = 0$ band in ^{50}Mn, respectively.

As a concrete example of recent data, the $N = Z + 2$ nucleus ^{50}Cr [6] and in its cross-conjugate ^{46}Ti [18,7] are presented in the following sections.

3 The nucleus ^{50}Cr

An updated level scheme at low excitation energy is reported in fig. 1 [6]. Two more levels are included with respect to ref. [1]: *i.e.* the 5^+ at 3875 and the 6^+ at 3826 keV. The same reaction ^{28}Si + ^{28}Si at 115 MeV as in ref. [1] was used.

The low-spin levels shown on the left of figure are taken from ref. [19], as they were not observed in the present heavy-ion reaction. ^{50}Cr is of particular interest, because it has been the first case in this region, where the presence of two close-lying 10^+ levels provided evidence of the band crossing between the prolate gs band and a sideband, whose nature was still controversial, as in ref. [20] was suggested to be a high-K prolate one, while in ref. [21] to be a rotational aligned state.

The present calculations, performed using the interaction KB3G [22], slightly modified with respect the KB3 one [8,1], differ little from the previous ones for the yrast levels [1]. Very good agreement is achieved, as shown in fig. 2. The negative-parity levels, which are expected to be grouped in $K^\pi = 4^-$ and 1^- bands, have been discussed in ref. [1].

The K assignment is based on calculated electric and magnetic moments. The calculated g-factors of the yrare 4^+ and 6^+ levels are 1.33 and -0.12, certifying their $1f_{7/2}$ proton and neutron nature, respectively. In a prolate Nilsson scheme one obtains $K^\pi = 4^+$ and 6^+ bands by promoting a proton or a neutron from $[312]3/2^-$ to $[321]5/2^-$ and $[321]5/2^-$ to $[330]7/2^-$, respectively and coupling the unpaired nucleons to the maximum K. This assignment is also confirmed by the theoretical Q_s values, since they are large and positive, according to Form. 1. Calculations predict some K-mixing, which reproduces the observed interband transitions. One would expect $K^\pi = 1^+$ bands from an antiparallel coupling. Low-spin levels are in fact observed [19] and well predicted, but the states are probably quite mixed, owing to the high level density. When assuming $K = 0$ in eq. (1), the theoretical Q_t value of the gs band decreases with excitation energy in a rather smooth way. The sudden change of calculated sign of Q_s along the gs band at the yrast 10^+ state is well explained by the simultaneous alignment of proton and neutron pairs. For a 10^+ level belonging to the gs band, a value of $-20\,\mathrm{efm}^2$ would be expected, while for the head of a $K^\pi = 10^+$ band and deformation parameter $\beta \simeq 0.25$ [1] a value of $+60\,\mathrm{efm}^2$ would be predicted. The observed positive values for both close lying 10^+ levels is explained as due to a strong mixing between the two states. Experimental lifetimes showed that present calculations predict a too large mixing [1]. The FPD6 interaction gives rise to a lower mixing since it predicts a negative Q_s value for the upper 10^+ [20], as expected for the continuation of the gs band. The yrast 10^+ level, on the other hand, is calculated to have $Q_\mathrm{s} = 46\,\mathrm{efm}^2$ indicating a high-K value,

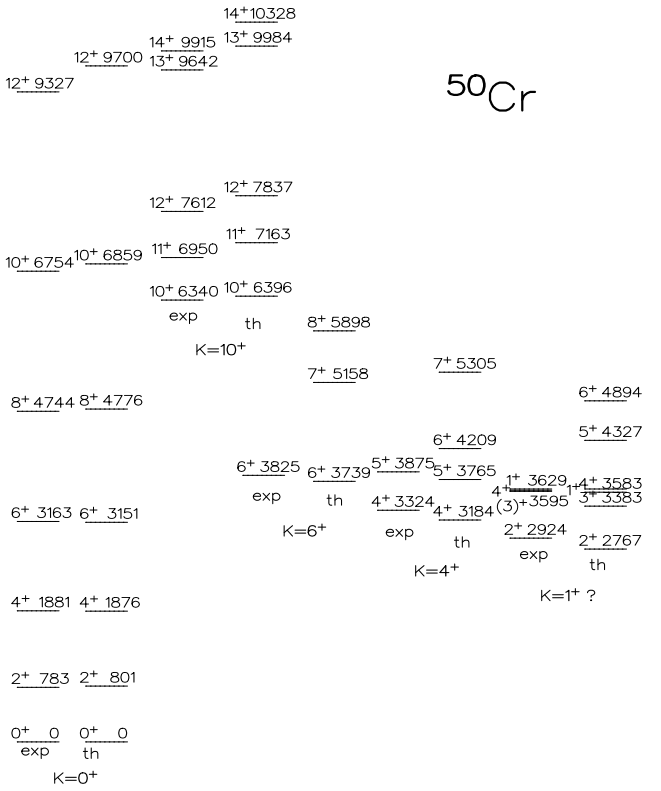

Fig. 2. Comparison of experimental and theoretical levels in ^{50}Cr, classified according to quantum number K.

according to eq. (1). Moreover, the 10^+ yrast level energy agrees roughly with the sum of the excitation energies of the yrare levels 4^+ and 6^+.

4 About Coulomb energy differences

The previous conclusions for the structure of ^{50}Cr can be compared with the observed Coulomb Energy Differences (CED) in the mirror pair ^{50}Fe-^{50}Cr [23], which are reported in fig. 3.

CED have been shown to be sensitive to the alignment of proton or neutron pairs. In fact, the breaking of a proton pair reduces the spatial overlap between the two protons and, most likely, of them with the rest of the nucleus. This reduces the Coulomb interaction and thus increases the binding energy, while in the mirror nucleus the corresponding neutron alignment does not affect the Coulomb energy. It must be pointed out, however, that they are not sensitive to the type of nucleon alignment: *i.e.* deformation alignment or rotational alignment in deformed nuclei, while in spherical nuclei one may get seniority-induced alignments.

It has been suggested, on the basis of CSM calculations [21], that rotational alignment occurs along the gs bands for nuclei in the middle of shell $1f_{7/2}$, but this is contradicted by the discussed case of ^{50}Cr, where essentially

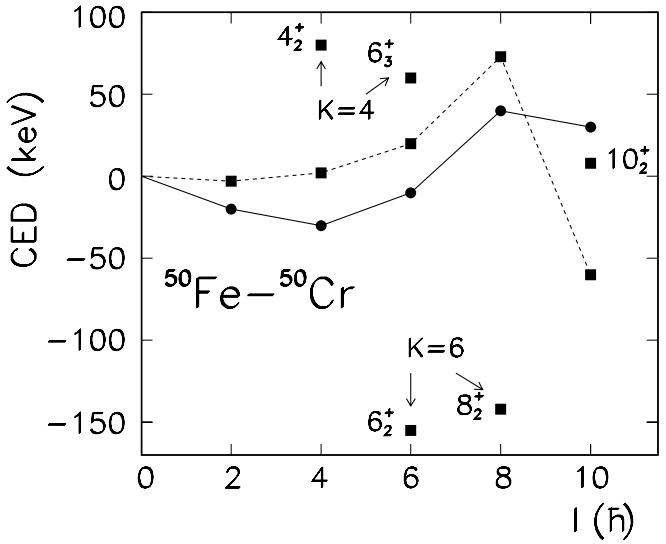

Fig. 3. Theoretical (squares) and experimental (circles) CED in ^{50}Fe-^{50}Cr.

strong coupling occurs, and the deformation alignment along the yrast band is a sudden phenomenon following band crossing with a multi-quasiparticle $K^\pi = 10^+$ band. The observed CED at $I^\pi = 10^+$ in the pair ^{50}Fe-^{50}Cr is mainly due to the alignment of two protons to $I = 6$ along the symmetry axis in ^{50}Fe, while the simultaneous alignment of two neutrons to $I = 4$ give rise to a smaller opposite effect. This is confirmed by the calculations reported in fig. 3, where a larger effect is calculated for the 6_2^+ state, than for the 4_2^+ one. It has to be noted that better agreement is obtained at $I = 10$ when additional contributions are considered [24].

In ^{51}Mn-^{51}Fe a similar sudden alignment occurs at $I = 17/2^-$ [25,26]. The $17/2^-$ level is isomeric, suggesting a change of shape, that can be associated with a sort of band crossing. An explanation similar to that in ^{50}Cr can be proposed. As some deformation ($\beta \simeq 0.25$) is observed below the $17/2^-$ level [19], the yrast $17/2^-$ level can be described as a $K^\pi = 17/2^-$ state, produced by the promotion of one nucleon from the $[321]5/2^-$ orbital to the $[330]7/2^-$ one and thus coupling all unpaired nucleons to the maximum K. This gives rise in ^{51}Fe to a proton pair alignment to $I = 6$ along the symmetry axis.

The explanation of CED in the gs band of ^{49}Mn-^{49}Cr seems to be different than in the ^{50}Fe-^{50}Cr case. The alignment is in this case smooth and the maximum CED effect is observed at $19/2^-$ [27]. This appears to be correlated with the observed backbending at $19/2^-$, which has been shown to be not due to a band crossing [2]. It is natural to ascribe it to similar effects as in ^{43}Sc and ^{53}Fe and thus to a seniority $v = 3$ effect. The fact that CED are smaller in ^{47}Cr-^{47}V [28] than in ^{49}Cr-^{49}Mn is probably correlated with the absence of backbending, which can be explained by the fact that neutron and proton-hole may drive ^{48}Cr to different shapes for ^{49}Cr and ^{47}V.

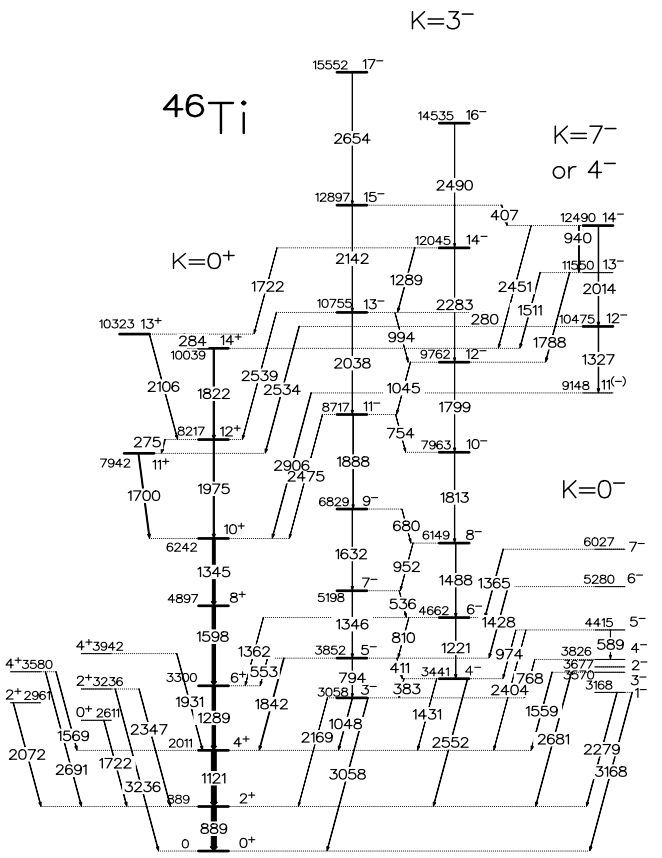

Fig. 4. Partial level scheme for ^{46}Ti.

5 The nucleus ^{46}Ti

The second nucleus illustrated is ^{46}Ti which is the cross conjugated of ^{50}Cr. The reaction ^{24}Mg(^{28}Si,α2p)^{46}Ti at 115 MeV was used, where, in order to perform a DSAM analysis, the target consisted of a 0.8 mg/cm^2 ^{28}Si foil backed either with Au or with Pb. An up-to-date level scheme is shown in fig. 4. No new levels were observed in the present measurement with respect to ref. [18], but the level scheme of fig. 1 includes also levels observed elsewhere. According to ref. [18], the gs band is reported up to band termination at $I = 14^+$. The low-spin positive-parity levels on the right were taken from [29]. The members of the previously known $K^\pi = 3^-$ band are reported up to the band termination 17^- in the $1d_{3/2}^{-1}1f_{7/2}^{n+1}$ configuration space [18]. This band is explained by the parallel coupling the $[202]3/2^+$ orbital to the $[321]3/2^-$ one. The antiparallel coupling gives rise to the negative-parity levels grouped in the $K^\pi = 0^-$ band, whose levels were taken from ref. [30,7]. The spin of levels at 3826 and 4415 keV are assigned as 4^- and 5^-, because the alternative assignments of 5^- and 6^- [31] are not compatible with observed lifetimes and decay schemes. The yrare levels 11^-, 12^-, 13^-, and 14^- are taken from ref. [18], but with the opposite parity, which is assigned from present lifetime measurements.

The gs band shows relevant differences with respect to the one in ^{50}Cr. The calculated energy levels are compared

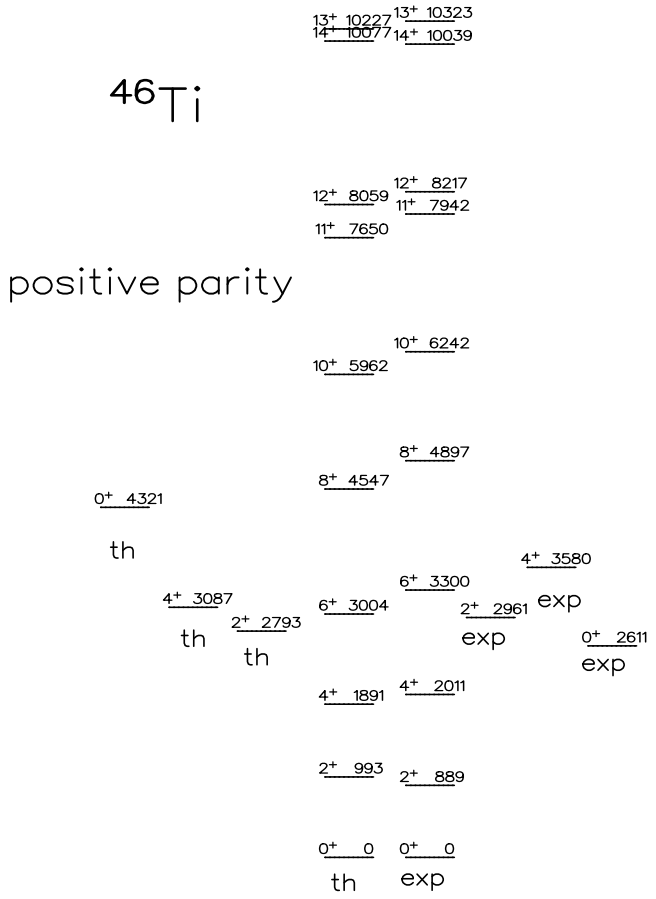

Fig. 5. Comparison between experimental and theoretical positive-parity levels in ^{46}Ti.

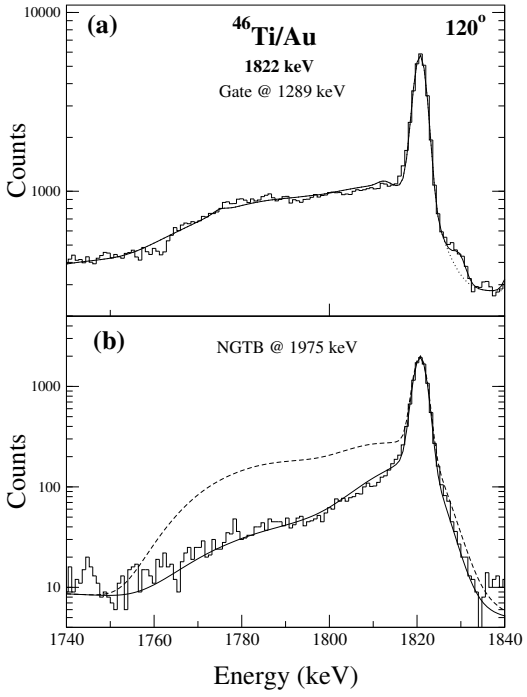

Fig. 6. NGTB lifetime analysis for the lifetimes associated with the $12^+ \rightarrow 10^+$, 1975 keV transition, using the $14^+ \rightarrow 12^+$ 1822 keV transition as a probe.

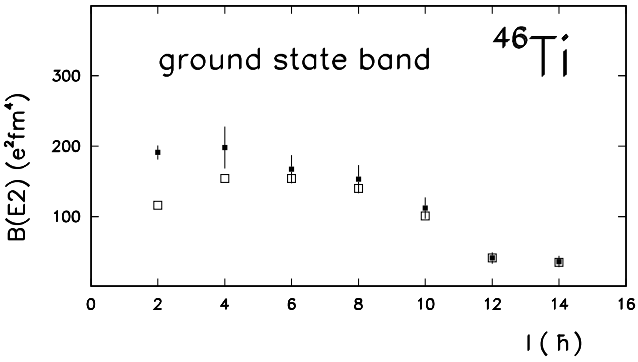

Fig. 7. $B(E2)$ rates for the gs band in ^{46}Ti.

with experimental ones in fig. 5. No band crossing occurs experimentally nor is predicted by LSSM. This is explained by noting that the bands formed using the Nilsson orbitals will have low K-value and thus cannot cross the gs band before its termination. This agrees with the fact that observed CED have a smooth behavior [32].

As an example, fig. 6 shows the NGTB analysis of the lifetime of the yrast 12^+ level in ^{46}Ti, which decays to the 10^+ via a 1975 keV transition. Taking the upper coincident transition as a probe, the comparison of its full lineshape with the partly suppressed lineshape, obtained taking a narrow gate on the lower transition, provides the lifetime associated to the gating transition.

Looking at fig. 7 one notes that the $B(E2)$ values for levels with spin larger than 4 are about 25% smaller indicating a smaller deformation than for ^{50}Cr. The fact that calculated values are sensibly smaller than experimental ones for 2^+ and 4^+ levels is ascribed to the mixing with highly deformed intruder states. In fact the comparison with LSSM in fig. 5 shows that the yrare 0^+ lies about 2 MeV lower than predicted. That level is thus interpreted as the band head of an intruder band built on $2h$- and $4h$-excitation in the $1d_{3/2}$ [33].

The comparison with SM predictions for negative-parity levels is shown in fig. 8. The lifetimes for the $K^\pi = 3^-$ band levels, not reported in this contribution, point to a deformation parameter $\beta \simeq 0.30$. The lifetimes of the $K^\pi = 0^-$ bands are being analysed in the reaction ^{7}Li(^{42}Ca, 2pn) [7]. Relying on theoretical calculations, the observed negative-parity sequence at high spin may have either $K^\pi = 4^-$ or 7^-, as a little change of the monopole part of the interaction may invert their relative position. The $K^\pi = 4^-$ band can be obtained by promoting a nucleon from the $[202]3/2^+$ to the $[312]5/2^-$ orbital, while the $K^\pi = 7^-$ one would be obtained by the simultaneous promotion of a proton from the $[202]3/2^+$ to the $[321]3/2^-$ orbital and of a neutron from the $[321]3/2^-$ to the $[312]5/2^-$ one.

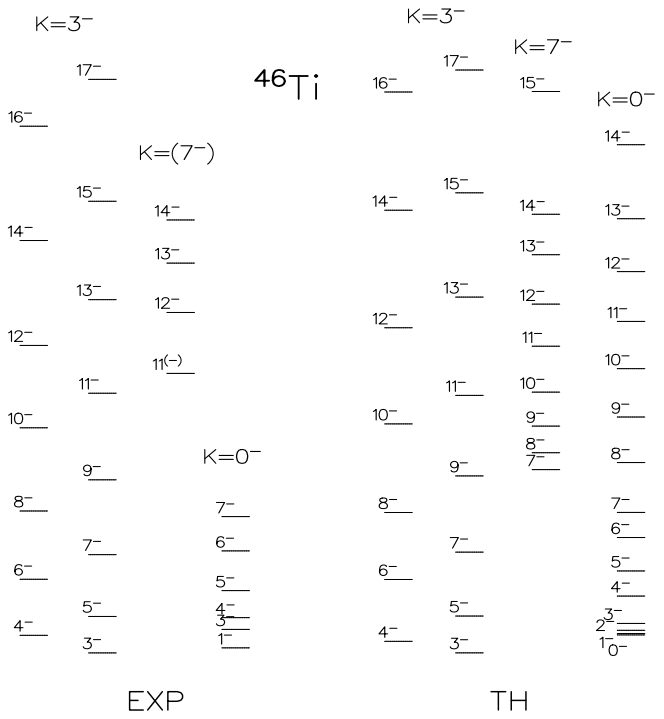

Fig. 8. Comparison between experimental and theoretical negative-parity levels in ^{46}Ti.

6 Summary

Recent results in ^{48}Cr, ^{49}Cr, ^{50}Cr, ^{47}V, ^{46}V, ^{48}V and ^{46}Ti nuclei are reviewed. A K-classification, based on strong-coupling description, turned out to be a good criterium to organise the level schemes at low spin both for natural and unnatural parity levels, indicating that there is not enough Coriolis coupling strength in the $1f_{7/2}$ shell to get substantial rotational alignment. Only the cases of ^{50}Cr and ^{46}Ti were discussed in detail. As compared with a previous work in ^{50}Cr [1], the description has been extended to non-yrast structures and evidence was found of two bands with $K^\pi = 4^+$ and 6^+, which are expected in a prolate Nilsson diagram, when breaking a proton and a neutron pair, respectively. Similarly, the yrast 10^+ level can be approximately described as a $K^\pi = 10^+$ state, due to the simultaneous breaking of proton and neutron pairs. It has been furthermore pointed out that the behaviour of CED for $1f_{7/2}$ nuclei can be consistently interpreted either in terms of a sudden band crossing with quasiparticle bands or with smooth alignment possibly related with the influence of the seniority scheme.

For ^{46}Ti preliminary data are reported. The influence on the gs band of an intruder band built on holes in the $1d_{3/2}$ orbital is established. The experimental level scheme is particularly rich for negative-parity levels. Apart from the known $K^\pi = 3^-$ band, also $K^\pi = 0^-$ and $K^\pi = (7)^-$ bands have been recognised, which are explained with strongly coupled Nilsson configurations.

Thank are due to the many co-authors of the quoted references, but in particular to J. Sánchez-Solano for the support with LSSM calculations.

References

1. F. Brandolini *et al.*, Nucl. Phys. A **642**, 387 (1998).
2. F. Brandolini *et al.*, Phys. Rev. C **60**, 041305 (1999).
3. F. Brandolini *et al.*, Nucl. Phys. A **693**, 517 (2001).
4. F. Brandolini *et al.*, Phys. Rev. C **64**, 044307 (2001).
5. F. Brandolini *et al.*, Phys. Rev. C **66**, 024304 (2002).
6. F. Brandolini *et al.*, Phys. Rev. C **66**, 021302 (2002).
7. F. Brandolini *et al.*, LNL Annu. Rep. 2001, p. 12 and submitted to Phys. Rev. C.
8. E. Caurier *et al.*, Phys. Rev. C **50**, 225 (1994).
9. E. Caurier *et al.*, Phys. Rev. Lett. **75**, 2466 (1995).
10. G. Martinez-Pinedo *et al.*, Phys. Rev. C **54**, R2150 (1996).
11. A. Zuker *et al.*, Phys. Rev. C **52**, R1742 (1995).
12. A. Poves, J. Sanchez-Solano, Phys. Rev. C **58**, 179 (1998).
13. F. Brandolini, R.V. Ribas, Nucl. Instrum. Methods A **417**, 150 (1998).
14. A. Juodagalvis, S. Åberg, Phys. Lett. B **428**, 227 (1998).
15. A. Juodagalvis *et al.*, Phys. Lett. B **477**, 66 (2000).
16. K. Hara *et al.*, Phys. Rev. Lett. **83**, 1922 (1999).
17. G. Martinez-Pinedo *et al.*, Phys. Rev. C **55**, 187 (1997).
18. D. Bucurescu *et al.*, Phys. Rev. C **67**, 034306 (2003).
19. T.W. Burrow, Nucl. Data Sheets **75**, 1 (1995).
20. L. Zamick, D.C. Zheng, Phys. Rev. C **54**, 956 (1996).
21. J.A. Sheikh *et al.*, Phys. Lett. B **443**, 1 (1998).
22. A. Poves *et al.*, Nucl. Phys. A **694**, 157 (2001).
23. S.M. Lenzi *et al.*, Phys. Rev. Lett. **87**, 122501 (2001).
24. A.P. Zuker *et al.*, Phys. Rev. Lett. **89**, 142502 (2002), nucl-th/0204053.
25. J. Ekman *et al.*, Eur. Phys. J. A **9**, 13 (2000).
26. M.A. Bentley *et al.*, Phys. Rev. C **62**, 051303 (2000).
27. C.D. O'Leary *et al.*, Phys. Rev. Lett. **79**, 4349 (1997).
28. M.A. Bentley *et al.*, Phys. Lett. B **437**, 243 (1998).
29. S.-C. Wu, Nucl. Data Sheets **91**, 1 (2000).
30. G.D. Dracoulis *et al.*, J. Phys. G **4**, 1323 (1978).
31. J.A. Cameron *et al.*, Phys. Rev. C **44**, 1882 (1991).
32. P.E. Garrett *et al.*, Phys. Rev. Lett. **87**, 051303 (2001).
33. W.J. Gerace, A.M. Green, Nucl. Phys. A **113**, 641 (1968).